HHS Public Access

Author manuscript

Gene Ther. Author manuscript; available in PMC 2020 July 22.

Published in final edited form as:

Gene Ther. 2014 June ; 21(6): 566–574. doi:10.1038/gt.2014.29.

Exploitation of Langerhans cells for *in vivo* DNA vaccine delivery into the lymph nodes

Enikő R. Tőke, PhD[1,7], **Orsolya Lőrincz, MSc**[1,7], **Zsolt Csiszovszki, PhD**[1,7], **Eszter Somogyi, PhD**[1,7], **Gabriella Felföldi, PhD**[1,8], **Levente Molnár, MSc**[1,7], **Róbert Szipőcs, PhD**[2], **Attila Kolonics, PhD**[2], **Bernard Malissen, PhD**[3], **Franco Lori, PhD**[4,7,9], **Jeffrey Trocio, MPH**[4,10], **Nyasha Bakare, MD**[4,11], **Ferenc Horkay, PhD**[5], **Nikolaus Romani, PhD**[6], **Christoph H. Tripp, PhD**[6], **Patrizia Stoitzner, PhD**[6], **Julianna Lisziewicz, PhD**[1,7,*]

[1]Genetic Immunity Kft, H-1045 Budapest, Berlini u. 47-49., Hungary

[2]Wigner RCP of HAS, H-1121 Budapest, Konkoly Thege út 29-33, Hungary

[3]Centre d'Immunologie de Marseille-Luminy, INSERM U1104, CNRS UMR7280, Aix Marseille Université, Marseille, France

[4]Research Institute for Genetic and Human Therapy (RIGHT), Bethesda, Maryland, USA

[5]Section on Tissue Biophysics and Biomimetics, Eunice Kennedy Shriver National Institute of Child Health and Human Development, NIH, Bethesda, Maryland 20892, USA

[6]Department of Dermatology & Venereology, Innsbruck Medical University, Innsbruck, Austria

[7]Present address: eMMUNITY Inc., 4400 East West Hwy, Bethesda MD 20814

[8]Present address: Egis Gyógyszergyár Nyrt. H-1106 Budapest, Keresztúri út 30-38., Hungary

[9]Present address: ViroStatics srl, 07100 Sassari, Italy

[10]Present address: Department of Outcomes Research, Pfizer Inc, New York, NY, USA

[11]Present address: Janssen Research and Development LLC, Titusville, NJ, USA.

Abstract

There is no clinically available cancer immunotherapy that exploits Langerhans cells (LCs), the epidermal precursors of dendritic cells that are the natural agent of antigen delivery. We developed a DNA formulation with a polymer and obtained synthetic ‘pathogen-like’ nanoparticles that preferentially targeted LCs in epidermal cultures. These nanoparticles applied topically under a patch elicited robust immune responses in human subjects. To demonstrate the mechanism of action of this novel vaccination strategy in live animals we assembled a high-resolution two-photon-laser-scanning-microscope. Nanoparticles applied on the native skin poorly penetrated and poorly induced LC-motility. The combination of nanoparticle administration and skin treatment was essential both for efficient loading the vaccine into the epidermis and for potent activation of the LCs to migrate into the lymph nodes. LCs in the epidermis picked up nanoparticles and

[*]Corresponding author: julianna.lisziewicz@emmunityinc.com; eMMUNITY Inc., 4400 East West Hwy Bethesda MD 20814.

Conflict of interest: JL, ET, CZ, OL, ES, LM, FL hold shares in Genetic Immunity Inc

Supplementary information is available at Gene Therapy’s website.

accumulated them in the nuclear region demonstrating an effective nuclear DNA delivery *in vivo*. Tissue distribution studies revealed that the majority of the DNA was targeted to the lymph nodes. Preclinical toxicity of the LC-targeting DNA vaccine was limited to mild and transient local erythema caused by the skin treatment. This novel, clinically proven LC-targeting DNA vaccine platform technology broadens the options on dendritic cell-targeting vaccines to generate therapeutic immunity against cancer.

Keywords

Langerhans cell; dendritic cell; nanomedicine; cancer immunotherapy; topical administration

INTRODUCTION

Innovative vaccines to treat cancer are designed to target dendritic cells (DC), the main inducers and regulators of the immune system[1]. Epidermal Langerhans cells (LCs) are dendritic cells specialized in the delivery of antigens to lymph nodes in order to induce cytotoxic Tlymphocytes (CTL) capable of specific killing of tumor cells[2,3,4,5,6]. Relatively few vaccines are administered to the epidermis and there is no vaccine that effectively and selectively targets the LCs before they migrate to the lymph nodes[7]. Vaccines that express antigens from a plasmid DNA (pDNA) do not require cross-priming to induce CTL responses. Therefore, preferential delivery of pDNA to LCs may result in more robust CTL responses than priming these cells with peptides or proteins[7,8]. Unfortunately, inefficient uptake and intracellular degradation of pDNA limits the efficacy of both antigen expression and induction of CTL responses[9].

We present here the mechanism of action of a clinically proven vaccine technology platform that was developed to harness the immunological function of LCs, to transport antigens from the periphery into the lymph nodes, and induce robust CTL responses. The underlying premise of this approach is provided by *ex vivo* manipulation of the DCs that generates optimally activated antigen presenting cells and a superior method for stimulating clinically significant antitumor and antiviral immunity as compared with more traditional vaccination methods. The platform technology has two key components: (1) LC-targeting nanoparticles that optimized for cellular entry and nuclear delivery of the pDNA for potent expression of antigens; (2) the nanoparticle vaccine formulation is combined with a medical device developed for *in vivo* LC-targeting vaccination. The first LC-targeting vaccine (DermaVir) was safe and induced potent and long-lasting memory CTL responses in human subjects as tested in three clinical trials for infectious disease indications[10,11,12]. Any DNA incorporated into nanoparticles would induce similar antigen-specific CTL responses because the physico-chemical properties of the LC-targeting nanoparticles are independent on the sequence and size of the encapsulated pDNA[13]. Our translational studies bring corroborating evidences that this technology safely and efficiently deliver pDNA-encoded antigens to the nucleus of LCs, increases their activation and their motility, facilitating antigen delivery to the lymph nodes. Finally, we demonstrate practical and inexpensive clinical applications of the LC-targeting vaccine as an *in vivo* alternative to dendritic cell-targeted immunotherapy developed against infectious, neoplastic and autoimmune diseases.

RESULTS

The size distribution of the vaccine

To develop a new DNA vaccine formulation we have encapsulated the pDNA within a linear polyethylenimine that is modified by covalently bound mannobiose molecules (polyethylenimine-mannose, PEIm) and hypothesized that these pDNA/PEIm nanoparticles are suitable for targeted pDNA delivery to LCs[13]. We investigated the size distribution of these nanoparticles by dynamic light scattering and atomic force microscopy. Size distribution of the Alexa-labeled nanoparticles was comparable to the non-labeled ones. They had a bimodal size distribution profile with two discrete size-ranges between 50-100 nm and 160-240 nm (Supplementary Fig. 1a, b).

Langerhans cells preferentially capture the vaccine

Ex vivo cultures of murine epidermal cells were employed to investigate the uptake of the nanoparticles by LCs. Alexa-546 labeled nanoparticles added to the cell culture were captured by more than 90% of the MHC class II positive LCs. These LCs become activated by the nanoparticles because they expressed the costimulatory molecule CD40 (Fig. 1b). In contrast, keratinocytes were inefficiently loaded with nanoparticles and epidermal T cells were devoid of nanoparticles (Fig. 1). The nanoparticles had undetectable cytotoxicity. These results indicate that LCs preferentially capture the nanoparticles.

Transgene expression in LCs was investigated by nanoparticles made with a pDNA encoding the Green Fluorescent Protein (GFP). These nanoparticles were applied onto the prepared skin of BALB/c mice, and then isolated epidermal cells were analyzed by flow cytometry (Table 1). In the negative control samples, 0.3 *%* of the cells were green. In the positive control, subcutaneous injection of FITC-dextran resulted in 15.9 % green cells[14]. For mice treated with the pDNA/PEIm nanoparticles on the surface of the skin, 9.4 % of the cells expressed GFP. After subcutaneous injection of the nanoparticles only 0.8 % of the cells expressed GFP. These data suggest that the pDNA/PEIm nanoparticles effectively transduce LCs after topical administration and poorly after injection[15].

Loading the vaccine into the epidermis

For LC-targeting vaccination we needed to deliver the nanoparticles to the proximity of LCs in the epidermis. We applied Alexa-514-labeled nanoparticles on either exfoliated or intact dorsal BALB/c mouse skin and three hours later we examined the different layers of the skin with scanning two-photon (2P) absorption fluorescence microscopy (Fig. 2). In the intact (shaved) skin most of the nanoparticles remained on the surface, albeit a small fraction penetrated into the upper layers of the epidermis. We found that exfoliation facilitated the penetration of nanoparticles into the epidermis. These nanoparticles formed a deposit at a depth of 50 to 110 pm. These experiments showed that skin exfoliation and barrier disruption is essential for efficient loading of the nanoparticles into the epidermis, in the close proximity of LCs.

Visualization of the Langerhans cell-targeting vaccination in live animals

We have assembled a non-invasive device suitable to examine the fate of the nanoparticles inside the skin *in vivo*. This is a near infrared (NIR) 2P absorption fluorescence laser scanning microscope (TPLSM) used in combination with advanced image analysis software. For visualization of the LCs in the skin of a living animal we used a knock-in mouse model expressing enhanced green fluorescent protein (eGFP) under the control of the Langerin (CD207) gene[16]. We established that the 2P emission of Alexa-546-labeled nanoparticles excited at wavelength of $\lambda_0 \sim 890$ nm is optimal at 550-600 nm ("red" non-descanned (NDD) channel) and marginal at 500-550 nm ("green" NDD channel). During our initial experiments we found that the eGFP signals of LCs are not detectable in the "red" NDD channel, suggesting that the green emission of LCs does not disturb the detection of the red emission of the nanoparticles (Fig. 3a).

We compared the images of LC-containing layers of intact and exfoliated epidermis with images of epidermis three and 24 hours after administration of nanoparticles. We observed that LCs in intact skin displayed thin and branched dendrites as described earlier (Fig. 3a)[16]. Notably, most LCs in intact skin specifically captured nanoparticles that penetrated through the epidermis (Fig. 3b). This result confirmed our previous observations indicating that a small amount of nanoparticle could penetrate intact skin (Fig. 2). The morphology of nanoparticle-loaded LC in the intact skin did not remarkably changed over a period of 24 hours. LC activation and nanoparticle uptake was different in the exfoliated skin. All LCs in the exfoliated skin picked up nanoparticles. Three hours after skin treatment LCs presented the classical dendritic morphology that changed to a more rounded, less branched phenotype after 24 hours, in accordance with previous data on tape-stripping (Fig. 3c)[16]. Interestingly, three hours after nanoparticle administration onto the exfoliated skin all LCs underwent significant morphologic changes showing rounded cell bodies with fewer, thicker, shorter and non-branched dendrites, a sign of motility and activation (Fig. 3d). This occurred at least 21 hours faster compared with skin exfoliation alone, without nanoparticle administration. Moreover, skin exfoliation increased the uptake of nanoparticles. The amount of nanoparticles in the LCs was greater in the exfoliated skin compared with the intact skin (Fig. 3e vs. Fig. 3f). We did not observe nanoparticles in any of the surrounding cells (e.g. keratinocytes). These results demonstrate the specificity of the LC-targeting vaccination. In addition, these high-resolution images demonstrated the first time perinuclear/nuclear localization of the nanoparticles in LCs suggesting that targeted delivery of pDNA into the nucleus of LCs was achieved *in vivo* (Fig. 3e and f). Our data suggest that the combination of skin exfoliation and nanoparticle administration is required for both optimal LC-targeting DNA delivery and optimal activation of LCs to migrate to the lymph nodes.

Topical vaccination increases the migration of Langerhans cells

Z-stack analysis of the epidermis with TPLSM is suitable for the *in vivo* detection of the initiation of LCs migration to the lymph nodes. For these migration studies 3D image stacks were acquired every 6 min for 48 min using 14 sections in a 28 μm penetration depth. We investigated the vertical movement of LCs by analyzing the appearance or disappearance of LCs in the same skin layer at different time points (Fig. 4a and b). Our results confirmed previous observation indicating that most of the LC was resident in the intact and in the

exfoliated skin. In contrast, exfoliation and nanoparticle administration together five-fold increased the motility of LCs. LC migration was documented by the appearance or disappearance of about 48% (SD = 22 %) of LCs in 38 minutes, in the observed zone. Interestingly, nanoparticle administration on intact skin also resulted in a two-fold increase of LC motility suggesting that the process of nanoparticle capture alone may provoke the migration of LCs (Fig. 4b).

To characterize the migration kinetics of vaccine-loaded LCs we developed a software that calculates the merged intensities (yellow) of eGFP and Alexa-546 fluorescence at every skin layer and every time points. Figure 4c demonstrates the vaccine-loaded LC within skin layers in consecutive time points, where the fluorescent intensity is proportional with the number of vaccine-loaded LC, the depth is the distance of the analyzed skin layer from the surface, and the time points represent the time after vaccine application. The analysis revealed that vaccine-loaded LC migrated into the deeper layers of the skin as demonstrated a shift of the maximum intensities in time from the upper layers of the skin toward the deeper layers. The ~20% decrease of fluorescent intensity in the upper layers of the skin indicate that vaccine-loaded LCs were rapidly exiting from the skin. Quantitative analysis showed that ~30% of vaccine-loaded LC left the skin in 48 minutes after vaccination (Supplementary Figure 2).

These results demonstrate that the combination of exfoliation and nanoparticle administration is required for the potent initiation of migration of the vaccine-loaded LCs to the lymph nodes.

Localization of the DNA in draining lymph nodes

We investigated the tissue distribution of the pDNA after LC-targeting vaccination in New Zealand White Rabbits 7, 30 and 60 days after treatment (Fig. 5). Seven days after a single topical application of the nanoparticles to the exfoliated skin 56% of the penetrated nanoparticles (average 421 pDNA copies/100 ng chromosomal DNA; SD% = 127) were detected in the skindraining lymph nodes (axillary, popliteal, inguinal, iliac, mesenteric lymph nodes) suggesting that nanoparticle-loaded LCs migrated to the lymph nodes (Fig. 5a). These results confirm and quantify our previous findings on expression of antigens encoded on pDNA in the lymph nodes of mice and macaques[17]. We found 32% of the nanoparticles (average 158 copies/100 ng DNA; SD% = 222) in the treatment-site muscle. This amount might reflect a contamination of the muscle with nanoparticles during the removal of the skin. Nanoparticles were undetectable in bone marrow suggesting that cells in the dermis, especially neutrophils, are not involved in the uptake of nanoparticles[18]. Nanoparticle distribution in plasma, whole blood, kidney, heart, brain, thymus, spleen, lung, liver, and genitalia ranged from 0.3 to 6 %. A separate rabbit cohort was sacrificed 30 days after LC-targeted vaccination. In these rabbits, the same tissue distribution pattern was observed despite decreased tissue pDNA levels. 47% of the penetrated nanoparticles were detected in the lymph nodes (average 36 pDNA copies/100 ng DNA; SD% = 105). The quantity of detectable nanoparticles further decreased after 60 days, with only sporadic weak positive signals detectable in the lymph nodes (average 17 pDNA copies/ 100 ng DNA; SD % = 200). No pDNA was detected in the control animals at any time. The calculated *in vivo*

half-life of the nanoparticles in the lymph nodes was 11.4 days indicating that the pDNA does not persist in the lymphoid tissues (Fig. 5b).

Clinical translation of Langerhans cell targeting vaccination

For the animal experiments we used sedated animals for skin treatment and to administer the liquid nanoparticles on the skin surface. For human use, we needed a mechanism that maintained the contact between the prepared epidermal surface and the vaccine. We developed a new medical device, called DermaPrep, indicated for topical administration of liquid formulations including the LC-targeting vaccine described here. It consists of three components assembled in a pouch: a body sponge (same material as used for mice and rabbits), medical tape and an 80 cm^2 transparent film dressing (patch). Each component has well-defined functions to facilitate a mild epidermal injury in the absence of scar formation, critical for efficient loading of the vaccine into the epidermis. Liquid vaccine administered under the patch are completely dried after three hours, potentially improving the degree of penetration seen in the animal experiments where the liquid nanoparticles were dried within 30 minutes without the use of the patch. Administration of the liquid vaccine with DermaPrep consists of 4 steps: reproducible and standardized epidermis preparation, patch application, loading of the liquid vaccine under the patch, and patch removal (Fig. 6).

Regulatory agencies require preclinical safety testing of the LC-targeting vaccination prior to clinical trials. We performed two placebo-controlled studies on New Zealand White Rabbits that included four and eight consecutive vaccine administrations with DermaPrep (Supplementary. Figure 3). The primary observation after four treatments was local skin irritation with slight erythema (Draize score grade 1 in <50% of total skin sites) and well-defined erythema (Draize score grade 2 in < 5% of total skin sites) (Supplementary Figure 3a, b)[19]. There were no differences between erythema severity observed immediately following skin treatment and 3 hours after patch removal, suggesting that skin treatment caused the desired slight epidermal injury. No edema was observed (Draize score grade 0; in 98 to 100% of total skin sites). Similar results for erythema and edema severity and occurrence rates were observed after 8 vaccine doses (Supplementary Figure 3c, d). Erythema was transient with recovery occurred within 24 to 72 hours. Interestingly, the skin recovery periods were shorter for subsequent LC-targeting vaccinations. The epidermis required 72 hours to fully recover following the first topical vaccination. After the second and third vaccinations, all skin sites recovered to normal within 48 and 24 hours, respectively. The recovery period remained 24 hours following the fourth and subsequent vaccinations (Supplementary Figure 3e).

All the animals exhibited slight body temperature increases following patch removal. There were no changes in body weight, food consumption, ophthalmologic effects, autoantibody responses, urinalysis, gross necropsy examinations, or organ weights. There were no apparent systemic blood chemistry or hematology toxicities.

DISCUSSION

We demonstrated the mechanism of action of the clinically proven LC-targeting DNA vaccination technology in *ex vivo* epidermal cell cultures and *in vivo* in live animals. We

showed that both skin exfoliation and nanoparticle administration were required for optimal loading of the vaccine into the LC and for potent activation of the vaccine-loaded LC to migrate into the lymph nodes. Biodistribution studies demonstrated half of the penetrated vaccine in the draining lymph nodes. Preclinical safety studies on repeated vaccinations on the same skin sites showed transient erythema as the major side effect.

We demonstrated that 50-240 nm size-range of the pDNA/PEIm nanoparticles, corresponding to the size-range of viruses, supports receptor mediated entry to LCs [13,20]. The mannose residues on the surface of these nanoparticles also resemble the surface of viruses that carry similar glycoprotein residues recognized by LCs[21]. This vaccine effectively penetrated into the epidermis after a mild skin exfoliation and formed a deposit. Unexpectedly, preferential and efficient uptake of the nanoparticles by LCs occurred not only in the exfoliated but also in the intact mouse skin. These findings might be explained by the bimodal size distribution of the nanoparticles with different penetration capability, and/or by the function of the LCs to sample the environment to pick up pathogens including mannosylated nanoparticles[22,23]. However, because human stratum corneum has a greater thickness compared with the mouse one, it is unlikely that these nanoparticles could also penetrate into the intact human skin[24].

Nanoparticle uptake by LCs is only part of the complex mechanism of vaccine delivery to the lymph nodes *via* LCs. We found that nanoparticles penetrated into the intact skin. LCs in the intact skin picked up the nanoparticles but they did not considerably change their morphology or motility. These results indicate that nanoparticle alone poorly stimulate LCs to mature and vaccine-loaded LC migration to the lymph nodes in the absence of exfoliation might be slow and inefficient. These results are in agreement with previous findings showing that pDNA/polyethyleneimine complexes remained at the vaccination site after delivery with either needle injection or Biojector® but these complexes are detectable in the lymph nodes after intravenous injection[25,26]. We demonstrated that skin preparation alone was not sufficient to induce rapid morphological changes of LCs, the first sign of motility. This is in good agreement with previous findings with tape stripping where LCs became motile after 16 hours, indicating that skin exfoliation is required to induce a mild skin injury (inflammation) and activate LCs to migrate to the lymph nodes[27].

Achieving migration of DCs into the lymph node represents one of the main challenges for cancer vaccines because antigen expression in the lymph nodes is necessary to induce effective CD8+ and CD4+ T cell responses. Here we demonstrated potent transgene expression in epidermal LCs after topical application of the nanoparticles. These data confirmed previous studies showing transgene expression in lymph nodes with RT-PCR, *in situ* hybridization and immunohistochemistry in mice and macaque models[17]. LC-targeting DNA vaccines express in the lymph nodes the DNA-encoded antigens and present several hundreds of epitopes on the patients' HLA molecules for direct-priming of naïve T cells. In contrast, the very poor antigen expression in LCs obtained after injection suggests a different mechanism of action. Injected DNA vaccines are optimized for *in situ* protein expression at the injection site[17]. DCs pick up the expressed proteins, similarly to injected protein vaccines, and cross-prime naïve T cells, consequently DNA could only be sporadically found in the lymph nodes[26,28]. Therefore, the direct-priming of CTL responses employed by

LC-targeting DNA vaccination seems to be superior to vaccination technologies that exploit cross-priming (gene gun, DNA injection, protein with adjuvants, etc.).

We clarified the mechanism of action in both *ex vivo* and *in vivo* settings demonstrating that nanoparticles-loaded LCs get activated in the skin to migrate into the lymph nodes. Previous studies showed that PEI-based nanoparticles upregulate the costimulatory markers of CD40 and CD86 *in vitro* and *in vivo* [29,30]. We found that all the LCs in epidermal cell culture captured the nanoparticles and expressed costimulatory molecules demonstrating the state of activation. This finding is supported with *in vivo* results showing phenotypic activation of nanoparticle-loaded LCs (Fig 3d). *In live animal* setting we showed that optimal LC activation and migration required both pDNA/PEIm formulation and topical administration of the nanoparticles after exfoliation of the skin.

Tremendous efforts have been put into the design of maturation cocktails mimicking pathogen-derived molecular activations[31]. The LC-targeting vaccination technology provides an *in vivo* solution to this challenge. We found that half of the penetrated vaccine was localized in the skin draining lymph nodes. Here we demonstrated that *in vivo* stimulation of LCs, with appropriate vaccine formulation and skin treatment, was required for the rapid initiation of migration of vaccine-loaded LCs to the lymph node. This observation further supports the potency of the vaccination technology mimicking the natural pathway for LC activation and consequent lymph node delivery of pathogen-derived antigens. Therefore, LC-targeting vaccination might improve the potent but cumbersome *ex vivo* dendritic cell-based vaccination methods used for infectious diseases and cancer treatment[32,33,34].

Many DNA vaccines proved to be immunogenic and effective in animal models but translation of these results to human vaccines have been unsuccessful. One common translational problem is that the vaccine dose administered to mice cannot be scaled up to humans. LC-targeting vaccination technology might solve this translation challenge by administering the vaccine topically onto the prepared skin. The skin has only a slightly variable Langerhans cell density in different mammals (a 900 to 1,800 cells/mm^{2}horizontal network under the skin surface)[35]. Therefore, the dose escalation can be achieved by targeting DNA to different lymph nodes simultaneously after applying the vaccine on differently sized and located skin surfaces[11].

There are concerns about the toxicity of pDNA/PEI nanoparticles[36]. Mortality was described in different strains of mice after intravenous administration of 50 μg pDNA nanoparticles[37]. Importantly, the LC-targeting pDNA/PEIm vaccine as safe as placebo and induced potent and long-lasting memory CTL responses in human subjects[11]. Therefore, toxicity obtained with different formulations and administration routes cannot be extrapolated. One reason for the conflicting toxicities observed might be due to the different PEIs used in nanoparticle formulations. These polymers can have either a branched- or linear-structure and a wide-range of molecular weights from 0.4 to 800 kDa. Another potential reason may be that the physiological salt concentration of the blood causes aggregation of the nanoparticles and drastically increases their size[12]. Such aggregation occurs after intravenous injection[38]. However, even under these circumstances, the 22 kDa molecular weight PEI used for the

formulation of pDNA/PEIm nanoparticles had lower toxicity than 800 kDa PEI[39,40]. Our studies demonstrated that DermaPrep skin preparation supported the safe and effective loading of the pDNA/PEIm nanoparticles into LCs. Two preclinical safety studies conclusively showed that toxicity of the LC-targeting vaccination was limited to a clinically acceptable mild erythema. These features make the LC-targeting vaccination technology a relevant CTL-inducing cancer vaccine product candidate in human subjects.

Vaccine development has entered into the era of rational design. The distinct functional capacities of different DC subsets are being harnessed41. By preferentially and effectively targeting antigens to LCs, a cell type critically implicated in CTL induction and anti-cancer immune responses, the described technology and approach holds promise for the future.

METHODS

Experimental design

Skin penetration studies in living animals: Nanoparticle penetration studies were performed on anesthetized Lang-EGFP mice (a knock-in mouse model expressing enhanced green fluorescent protein (eGFP) under the control of the Langerin (CD207) gene[16]). Skin samples were excised and were investigated by TPLSM for the presence of labeled nanoparticles in the epidermal cell layers as well as for the morphologic and motility changes of Langerhans cells induced by the nanoparticles (n=3).

Tissue distribution after topical delivery of nanoparticles: A single topical vaccine treatment was performed on 42 white New Zealand White Rabbits in a GLP study. 30 animals received nanoparticle solution containing pDNA encoding HIV genes (DermaVir) and 12 animals received control solution[41]. Animals were sacrificed on days 7, 30 or 60 for qPCR detection of pDNA distributed in organs and tissues. Four parallel qPCR reactions were made for each tissue sample.

Safety studies with topical vaccine treatment: Topical vaccine treatment was performed according to the human protocol (http://www.geneticimmunity.com/IFU) in a GLP study. Twenty New Zealand rabbits were treated with 0.8 mL nanoparticles in glucose solution under two patches. The control group received only glucose. Three (i.e., immediately after removal of the patch), 24, 48, and 72 hours after treatments the skin sites were graded by a blinded operator according to the Numerical Grading System for Treatment Site Irritation[19].

Preparation and characterization of the nanoparticles

PEIm (polyethyleneimine mannose containing 3% mannose residues calculated to amino groups) was labeled with Alexa-546 or −514 (Invitrogen, CA, USA). Nanoparticles were prepared with pDNA encoding HIV-1 genes of DermaVir[17] or pDNA encoding the Green Fluorescence Protein and PEIm as described previously[42]. Size distribution were performed with Brookhaven ZetaPALS™ at 25 °C. For atomic force microscopy (Bioscope I with Nanoscope IV controller, Veeco) the nanoparticle solution was dried on APS-mica. Imaging was made in air in tapping mode[13]. Based on previous AFM measurements the

polyethylenimine coats one molecule of pDNA, which means that 0.1 mg pDNA (12.5 kBp » 8 MDa) corresponds to 7.5×10^{12} nanoparticles, ie. the concentration of nanoparticles is 9.3 x 10^{12} nanoparticle/ml formulation[13].

Animals

General procedures for animal care and housing were in accordance with the National Research Council (NRC) *Guide for the Care and Use of Laboratory Animals* (1996) and the Animal Welfare Standards. Rabbits and mice were anesthetized using sodium pentobarbital administered intravenously or intraperitonally. TPLSM studies were approved by the Semmelweis University Animal Care and Use Committee.

Topical vaccination of mice

Topical vaccine treatment was performed according to the human protocol (http://www.geneticimmunity.com/IFU) using the same materials except transparent film (the patch): (a) The skin treatment starts with shaving and disinfection, then the body sponge is used to exfoliate the epidermis; (b) Tape stripping for the removal of the residual skin material (e.g.: dead cells); Liquid vaccine administered on the skin and left to completely dry for 30 minutes.

Epidermal cell culture, gene expression and flow cytometry

7 million murine epidermal cells were isolated and cultured with Alexa546-labeled nanoparticles as described previously[43]. After 20 h samples were stained using antibodies against MHC-class II (clone M5/114.15.2, eBioscience), CD40 (clone 3/23, Becton Dickinson) and CD45 (clone 30-F11, eBioscience) and analyzed on a FACSCantoII™ flow cytometer (Becton Dickinson). Dead cells were excluded by co-staining with 7AAD (Becton Dickinson). About 1 % of the MHC-class II positive cells were dead in the nanoparticle treated samples, and about 0.7% in the untreated controls. A minimum of 200,000 events was acquired for each measurement. FACS data were analyzed with FlowJo software.

For gene expression experiments six hours after skin preparation and nanoparticle administration, the mice were sacrificed, the skin was removed and cultured as described previously. The cells that migrated out from the skin into the culture media were harvested and the large cells containing the LC population were analyzed using flow cytometry.

Skin penetration studies with Z-stack analysis

For nanoparticle penetration studies anesthetized BALB/c mice were sacrificed after three hours of Alexa514-labelled nanoparticle treatment. Skin samples were excised and for 2P excitation of the Alexa-514 dye, a mode-locked Yb-fiber laser (λ_0 ~ 1030 nm, τ ~ 300 fs) was used. 3D image stacks were acquired (1500 x 1500 x 80 μm) using 10 sections and magnification of 40. Excitation was 1,030 nm.

Studies on living mice with femtosecond two-photon laser scanning microscope (TPLSM)

Anesthetized *Lang-EGFP* mice were laid on the heated microscope-table and the ears of mouse were fixed to microscope slide and examined with TPLSM that we have assembled. For 3D measurements a femtosecond pulse Ti-sapphire laser generates nearly transform

limited, rFWHM ~190 fs pulses at a repetition rate of ~76 MHz[44]. The laser utilizes ultra broadband chirped mirror technology for broad tunability (690 nm to 1050 nm) without changing the cavity optics. The laser central wavelength was set to ~910 nm, which assures high two-photon excitation efficiency for both the Alexa546-labelled nanoparticles and the eGFP-labelled LCs, but low background autofluorescence signal from the intrinsic autofluorescent molecules in the skin[43]. For 3D imaging, we used a two-channel, Axio Examiner LSM 7MP microscope (Carl Zeiss, Germany). Scanning in the x–y plane was achieved with galvanometer mirrors. Subfemtolitre excitation beam focusing was achieved using a high-numerical-aperture (N.A., 1.3) 40x water immersion objective (Zeiss), with a working distance of about 1 mm. Stepper motor control of the objective lens focus enabled scanning along the optical z-axis with a minimum step size of 150 nm. The average power of the laser beam reaching the sample is typically set to ~ 10 mW by a built-in acousto-optic device, which assures thermal-damage free excitation. For cross-talk free recording of the flourescence signals two bandpass filters and a corresponding dichroic filter were placed in front of the non-descanned detectors: a BPF1 (green) BPF2 (red) filters having transmission bands in the 500-550 nm and the 565-610 nm wavelength regimes.

For LC migration studies 3D image stacks were acquired every 6 min for 48 min using 14 sections, 28 μm skin penetration and a magnification of 40. For the estimation of vertical movement of LCs a percentage rate was established: count (sum) of the newly appearing and disappearing cells divided by the total number of cells observed in the field. LSM software was used for image processing.

Tissue distribution after topical delivery of nanoparticles

A single topical vaccine treatment was performed on 42 white New Zealand rabbits. 30 animals received 0.8 mL nanoparticle solution containing pDNA encoding HIV genes (DermaVir) and 12 animals received 0.8 mL of control solution[41]. Animals were sacrificed on days 7, 30 or 60 for qPCR detection of pDNA distributed in organs and tissues. Half-life is calculated following the equation: Half-life = (elapsed time*log2)/log(beginning amount/ending amount).

From 23 tissue samples per rabbit genomic DNA were purified (DNeasyQiagen, CA). Four parallel qPCR reactions were made for each tissue sample. The blank control was water. Detection limit was established as 10 copies/100ng genomic DNA. Primer1: 5’ATAATCCACCTATCCCAGTAGGAGAAAT3’; Primer2: 5’GGTCCTTGTCTTATGTCCAGAAxTGC 3’ where x is a Lightcycler Red640 flurophore; probe 5’TAAATAAAATAGTAAGAATGTATAGCCCTACCAGC-fl3’. Conditions: denaturing step for 10 min at 95°C, followed by 55 cycles of amplification (95°C for 10 sec, 55°C for 10 sec, 72°C for 5 sec), and ending with a melting cycle of continuous increase in temperature up to the target temperature of 80 °C.

Supplementary Material

Refer to Web version on PubMed Central for supplementary material.

ACKNOWLEDGEMENTS

The authors wish to thank Drs. Michael A Ussery and Hao Zhang (Division of AIDS, NIAID) for their support.

The study was supported by NIH (N01-AI-70043) and Hungarian National Office for Research and Technology (FIBERSC2 and DVCLIN01). F.H. acknowledges the support of the Intramural Research Program of the NICHD, NIH. C.H.T. was in part supported by the COMET Center ONCOTYROL (Cell Therapy Unit), which is funded by the Austrian Federal Ministries for Transport, Innovation and Technology, and Economics, Family and Youth (via the Austrian Research Promotion Agency / FFG) and the Standortagentur Tirol.

REFERENCES

1. Steinman RM. Decisions about dendritic cells: past, present, and future. Annual Review of Immunology 2012; 30: 1–22.
2. Stoitzner P, Green LK, Jung JY, Price KM, Tripp CH, Malissen B, et al. Tumor immunotherapy by epicutaneous immunization requires langerhans cells. Journal of Immunology (Baltimore, Md : 1950) 2008; 180: 1991–8.
3. Banchereau J, Thompson-Snipes L, Zurawski S, Blanck J-P, Cao Y, Clayton S, et al. The differential production of cytokines by human Langerhans cells and dermal CD14(+) DCs controls CTL priming. Blood 2012; 119: 5742–9. [PubMed: 22535664]
4. Romano E, Cotari JW, Barreira da Silva R, Betts BC, Chung DJ, Avogadri F, et al. Human Langerhans cells use an IL-15R-α/IL-15/pSTAT5-dependent mechanism to break T-cell tolerance against the self-differentiation tumor antigen WT1. Blood 2012; 119: 5182–90. [PubMed: 22510877]
5. Romani N, Thurnher M, Idoyaga J, Steinman RM, Flacher V. Targeting of antigens to skin dendritic cells: possibilities to enhance vaccine efficacy. Immunology and Cell Biology 2010; 88: 424–30. [PubMed: 20368713]
6. Zaric M, Lyubomska O, Touzelet O, Poux C, Al-Zahrani S, Fay F, et al. Skin Dendritic Cell Targeting via Microneedle Arrays Laden with Antigen-Encapsulated Poly-d,l-lactideco-Glycolide Nanoparticles Induces Efficient Antitumor and Antiviral Immune Responses. ACS Nano 2013. doi:10.1021/nn304235j.
7. Stoitzner P, Sparber F, Tripp CH. Langerhans cells as targets for immunotherapy against skin cancer. Immunology and Cell Biology 2010; 88: 431–7. [PubMed: 20351746]
8. Combadière B, Vogt A, Mahé B, Costagliola D, Hadam S, Bonduelle O, et al. Preferential amplification of CD8 effector-T cells after transcutaneous application of an inactivated influenza vaccine: a randomized phase I trial. PloS One 2010; 5: e10818. [PubMed: 20520820]
9. Diebold SS, Kursa M, Wagner E, Cotten M, Zenke M. Mannose polyethylenimine conjugates for targeted DNA delivery into dendritic cells. The Journal of Biological Chemistry 1999; 274: 19087–94. [PubMed: 10383411]
10. Lisziewicz J, Tőke ER. Nanomedicine applications towards the cure of HIV. Nanomedicine : Nanotechnology, Biology, and Medicine 2013; 9(1): 28–38.
11. Lisziewicz J, Bakare N, Calarota S a, Bánhegyi D, Szlávik J, Ujhelyi E, et al. Single DermaVir immunization: dose-dependent expansion of precursor/memory T cells against all HIV antigens in HIV-1 infected individuals. PloS One 2012; 7: e35416. [PubMed: 22590502]
12. Rodriguez B, Asmuth DM, Matining RM, Spritzler J, Jacobson JM, Mailliard RB, et al. Safety, tolerability, and immunogenicity of repeated doses of DermaVir, a candidate therapeutic HIV vaccine, in HIV-infected patients receiving combination antiretroviral therapy: results of the ACTG 5176 trial. Journal of Acquired Immune Deficiency Syndromes 2013; 64(4): 351–359. [PubMed: 24169120]
13. Lőrincz O, Tőke ER, Somogyi E, Horkay F, Chandran PL, Douglas JF, et al. Structure and biological activity of pathogen-like synthetic nanomedicines. Nanomedicine : Nanotechnology, Biology, and Medicine 2012; 8: 497–506.
14. Bruewer M, Utech M, Hopkins AM, Parkos C a, Nusrat A. Interferon-gamma induces internalization of epithelial tight junction proteins via a macropinocytosis-like process. FASEB

Journal : Official Publication of the Federation of American Societies for Experimental Biology 2005; 19: 923–33. [PubMed: 15923402]

15. Sallusto F, Cella M, Danieli C, Lanzavecchia A, Dendritic cells use macropinocytosis and the mannose receptor to concentrate macromolecules in the major histocompatibility complex class II compartment: downregulation by cytokines and bacterial products. Journal of Experimental Medicine 1995; 182(2): 389–400. [PubMed: 7629501]
16. Kissenpfennig A, Henri S, Dubois B, Laplace-Builhé C, Perrin P, Romani N, et al. Dynamics and function of Langerhans cells in vivo: dermal dendritic cells colonize lymph node areas distinct from slower migrating Langerhans cells. Immunity 2005; 22: 643–54. [PubMed: 15894281]
17. Lisziewicz J, Trocio J, Whitman L, Varga G, Xu J, Bakare N, et al. DermaVir: a novel topical vaccine for HIV/AIDS. J Invest Dermatol 2005; 124: 160–9. [PubMed: 15654970]
18. Duffy D, Perrin H, Abadie V, Benhabiles N, Boissonnas A, Liard C, et al. Neutrophils Transport Antigen from the Dermis to the Bone Marrow, Initiating a Source of Memory CD8+ T Cells. Immunity 2012; 37: 917–29. [PubMed: 23142782]
19. Draize JH, Woodard G, Calvery HO. Methods for the study of irritation and toxicity of substances applied topically to the skin and mucous membranes. J Pharmacol Exp Ther 1944; 82: 377–90.
20. Racoosin EL, Swanson J a. M-CSF-induced macropinocytosis increases solute endocytosis but not receptor-mediated endocytosis in mouse macrophages. Journal of Cell Science 1992; 102 (Pt 4: 867–80. [PubMed: 1429898]
21. Van der Vlist M, Geijtenbeek TBH. Langerin functions as an antiviral receptor on Langerhans cells. Immunology and Cell Biology 2010; 88: 410–5. [PubMed: 20309013]
22. Frugé RE, Krout C, Lu R, Matsushima H, Takashima A. Real-time visualization of macromolecule uptake by epidermal Langerhans cells in living animals. The Journal of Investigative Dermatology 2012; 132: 609–14. [PubMed: 22113485]
23. Kubo A, Nagao K, Yokouchi M, Sasaki H, Amagai M. External antigen uptake by Langerhans cells with reorganization of epidermal tight junction barriers. The Journal of Experimental Medicine 2009; 206: 2937–46. [PubMed: 19995951]
24. So P, Kim IK H. Two-Photon deep tissue ex vivo imaging of mouse dermal and subcutaneous structures. Opt Express 1998; 3: 339–50. [PubMed: 19384379]
25. Jeong G-J, Byun H-M, Kim JM, Yoon H, Choi H-G, Kim W-K, et al. Biodistribution and tissue expression kinetics of plasmid DNA complexed with polyethylenimines of different molecular weight and structure. Journal of Controlled Release : Official Journal of the Controlled Release Society 2007; 118: 118–25. [PubMed: 17250923]
26. Sheets RL, Stein J, Manetz TS, Duffy C, Nason M, Andrews C, et al. Biodistribution of DNA plasmid vaccines against HIV-1, Ebola, Severe Acute Respiratory Syndrome, or West Nile virus is similar, without integration, despite differing plasmid backbones or gene inserts. Toxicological Sciences : An Official Journal of the Society of Toxicology 2006; 91: 610–9. [PubMed: 16569729]
27. Kissenpfennig A, Henri S, Dubois B, Laplace-Builhé C, Perrin P, Romani N, et al. Dynamics and function of Langerhans cells in vivo: dermal dendritic cells colonize lymph node areas distinct from slower migrating Langerhans cells. Immunity 2005; 22: 643–54. [PubMed: 15894281]
28. Chen D, Payne LG. Targeting epidermal Langerhans cells by epidermal powder immunization. Cell Research 2002; 12: 97–104. [PubMed: 12118944]
29. Xun S, Simu Ch, Jianfeng H, Zhirong Zh Mannosylated biodegradable polyethyleneimine for targeted DNA delivery to dendritic cells. International Journal of Nanomedicine 2012; 7:2929–2942. [PubMed: 22745554]
30. Alshamsan A, Hamdy S, Haddadi A, Samuel J, El-Kadi AOS, Uludağ H, Lavasanifar A STAT3 Knockdown in B16 Melanoma by siRNA Lipopolyplexes Induces Bystander Immune Response In Vitro and In Vivo. Translational Oncology 2011; 4(3):178–188. [PubMed: 21633673]
31. Pilling AM, Harman RM, Jones SA, McCormack NAM, Lavender D, Haworth R. The assessment of local tolerance, acute toxicity, and DNA biodistribution following particlemediated delivery of a DNA vaccine to minipigs. Toxicologic Pathology; 30: 298–305. [PubMed: 12051546]
32. Garcia F, Climent N, Guardo AC, Gil C, León A, Autran B, et al. A Dendritic Cell-Based Vaccine Elicits T Cell Responses Associated with Control of HIV-1 Replication. Science Translational Medicine 2013; 5: 166ra2.

33. Strioga MM, Felzmann T, Powell DJ Jr, Ostapenko V, Dobrovolskiene NT, Matuskova M, et al. Therapeutic dendritic cell-based cancer vaccines: the state of the art. Critical Reviews in Immunology. 2013; 33(6): 489–547. [PubMed: 24266347]
34. Gilboa E DC-based cancer vaccines. The Journal of Clinical Investigation 2007; 117(5): 1195–1203. [PubMed: 17476349]
35. Bauer J, Bahmer F a, Wörl J, Neuhuber W, Schuler G, Fartasch M. A strikingly constant ratio exists between Langerhans cells and other epidermal cells in human skin. A stereologic study using the optical disector method and the confocal laser scanning microscope. The Journal of Investigative Dermatology 2001; 116: 313–8. [PubMed: 11180009]
36. Goula D, Remy JS, Erbacher P, Wasowicz M, Levi G, Abdallah B, et al. Size, diffusibility and transfection performance of linear PEI/DNA complexes in the mouse central nervous system. Gene Therapy 1998; 5: 712–7. [PubMed: 9797878]
37. Chollet P, Favrot MC, Hurbin A, Coll J-L. Side-effects of a systemic injection of linear polyethylenimine-DNA complexes. The Journal of Gene Medicine; 4: 84–91. [PubMed: 11828391]
38. Kircheis R, Wightman L, Wagner E. Design and gene delivery activity of modified polyethylenimines. Advanced Drug Delivery Reviews 2001; 53: 341–58. [PubMed: 11744176]
39. Wightman L, Kircheis R, Rössler V, Carotta S, Ruzicka R, Kursa M, et al. Different behavior of branched and linear polyethylenimine for gene delivery in vitro and in vivo. The journal of gene medicine 2001; 3: 362–72. [PubMed: 11529666]
40. Palucka K, Banchereau J, Mellman I. Designing vaccines based on biology of human dendritic cell subsets. Immunity 2010; 33: 464–78. [PubMed: 21029958]
41. Somogyi E, Xu J, Gudics A, Tóth J, Kovács AL, Lori F, et al. A plasmid DNA immunogen expressing fifteen protein antigens and complex virus-like particles (VLP+) mimicking naturally occurring HIV. Vaccine 2011; 29: 744–53. [PubMed: 21109034]
42. Toke ER, Lorincz O, Somogyi E, Lisziewicz J. Rational development of a stable liquid formulation for nanomedicine products. International Journal of Pharmaceutics 2010; 392: 261–7. [PubMed: 20347027]
43. Stoitzner P, Romani N, McLellan AD, Tripp CH, Ebner S. Isolation of skin dendritic cells from mouse and man. Methods in Molecular Biology (Clifton, NJ) 2010; 595: 235–48.
44. Mayer EJ, Möbius J, Euteneuer A, Rühle WW, Szip Cs R. Ultrabroadband chirped mirrors for femtosecond lasers. Optics Letters 1997; 22: 528–30. [PubMed: 18183256]
45. Breunig HG, Studier H, König K. Multiphoton excitation characteristics of cellular fluorophores of human skin in vivo. Optics Express 2010; 18: 7857–71. [PubMed: 20588627]

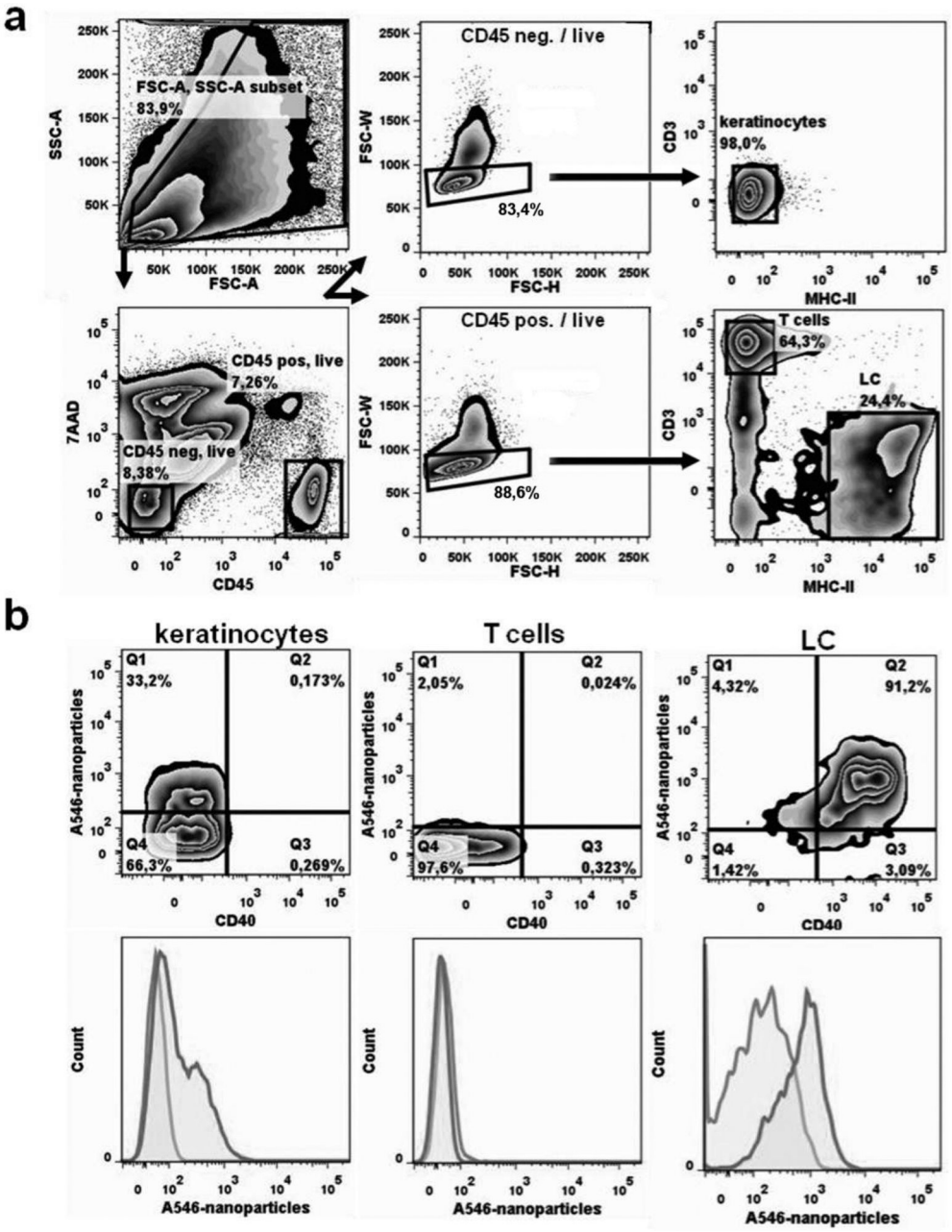

Figure 1. In vitro capture of pDNA/PEIm nanoparticles by LCs.

After skin preparation epidermal cell suspensions were isolated and incubated with Alexa-546-labeled nanoparticles (A546-nanoparticles). a) Representative FACS gating strategy. Arrows indicate the sequence of steps. First, cells are discriminated from debris on the basis of forward (FSC-A) and side scatter (SSC-A) characteristics (top left panel). Second, dead cells are excluded from further analysis by their 7AAD positivity (lower left panel). Third, within viable CD45-negative cells (i.e., keratinocytes; upper middle panel) and viable CD45+ cells (lower middle panel) doublets are identified by their FSC-W and FSC-H properties and are omitted from further analysis. Doublets are the cells outside the gated area; about 20%. Single cells (about 80%) are within the gate. Fourth, epidermal cells

are defined as MHC-II-/CD3- keratinocytes (upper right panel) and MHC- II+/CD3- Langerhans Cells and MHC-II-/CD3+ dendritic epidermal T cells / DETC (lower right panel). b) Representative FACS contour plots (upper row) and histogram overlays (lower row) of keratinocytes, dendritic epidermal T cells and CD40+ Langerhans cells show the uptake of nanoparticles. show the uptake of Alex-546-conjugated nanoparticles (dark grey lines) compared to control cultures without nanoparticles (light grey lines). Representative FACS plots are shown of 4 individually analysed mice per group.

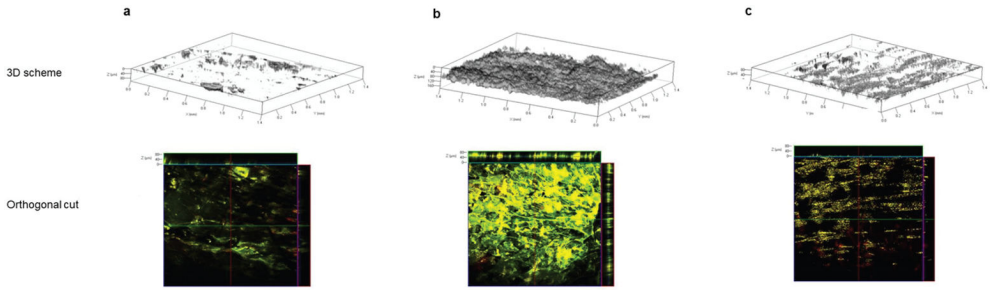

Figure 2. Penetration of pDNA/PEIm nanoparticles into the skin.

(**a**) Dorsal skin of control BALB/c mice without skin exfoliation and nanoparticle application; (**b**) Application of Alexa-514-labeled nanoparticle onto the surface of exfoliated dorsal skin of mice. Penetration depth is 50-110 μm; (**c**) Application of Alexa-514-labeled nanoparticles onto the surface of shaved skin. Penetration depth is 1-40 μm.

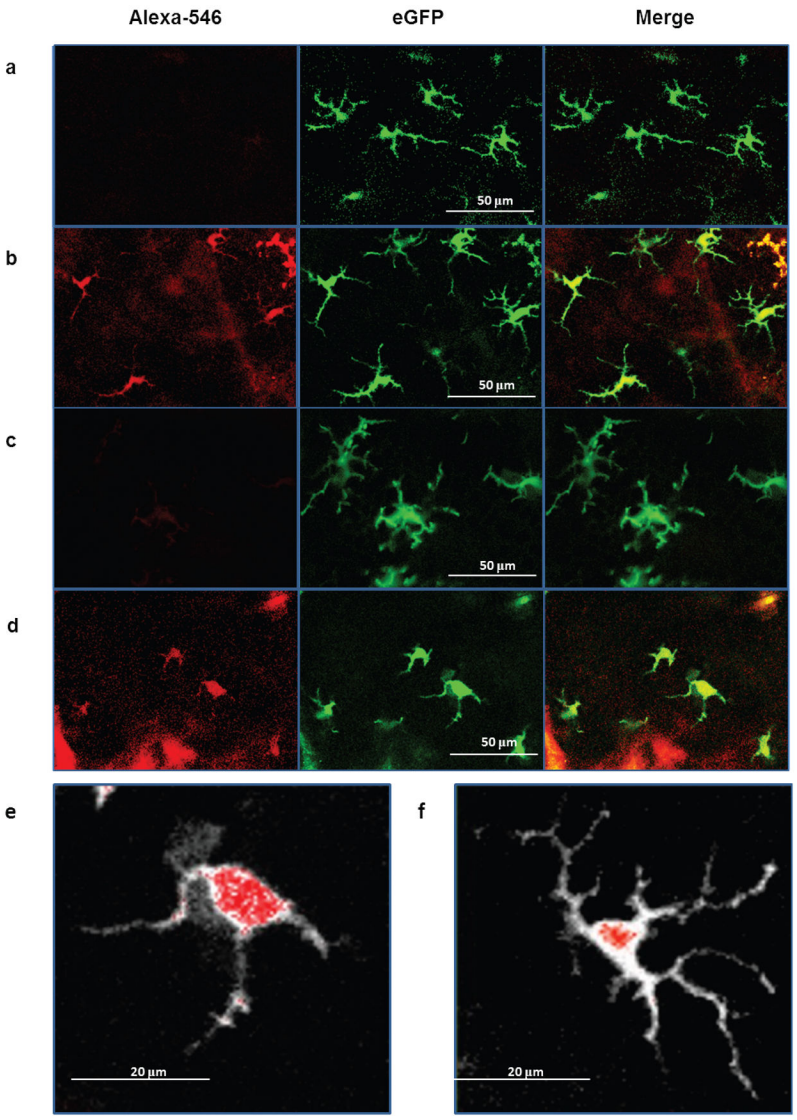

Figure 3. Real time visualization of the incorporation of Alexa-546-labeled nanoparticles by LCs in living eGFP-Langerin knock-in mouse after 3 hours.

(**a**) control (intact) skin; (**b**) nanoparticles applied onto intact skin; (**c**) exfoliated skin; (**d**) nanoparticles applied onto exfoliated skin; (**e-f**) images showing the morphology of representative LCs (white) with nanoparticles (red) (**e**) a motile LC with nanoparticles after skin exfoliation; (**f**) resident LC with nanoparticles in intact skin. The green channel was gray scaled and the red channel was merged with the gray image.

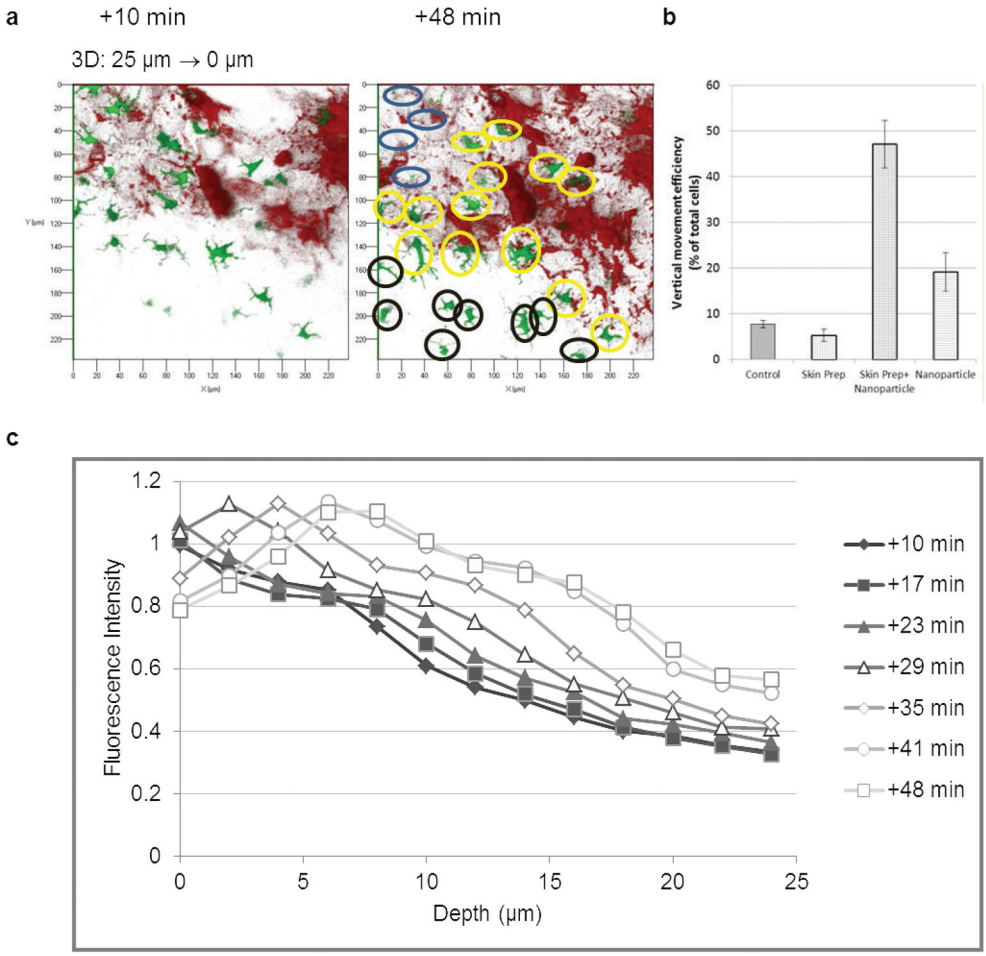

Figure 4. Motility of LCs in the epidermis of eGFP-Langerin knock-in mouse after 2 hours.

(a) The representative Z-stack layer of a mouse skin +10 and +48 minutes after skin exfoliation and nanoparticle administration demonstrating an example for the vertical movement of LCs. Analysis were performed by counting the appearing (black circles), disappearing (blue circles) and remaining cells (yellow circles) after +48 min compared with the cells present in the same skin +10 minutes. Field: 240 µm x 240 µm; **(b)** Vertical movement efficiency of LCs after different treatments; **(c)** Migration kinetics of nanoparticle-loaded LCs after combined administration of skin treatment and nanoparticles. Merged intensities (yellow) of eGFP (green) and Alexa-546 (red) were calculated in every Z-axis profile at every time point, representing each line.

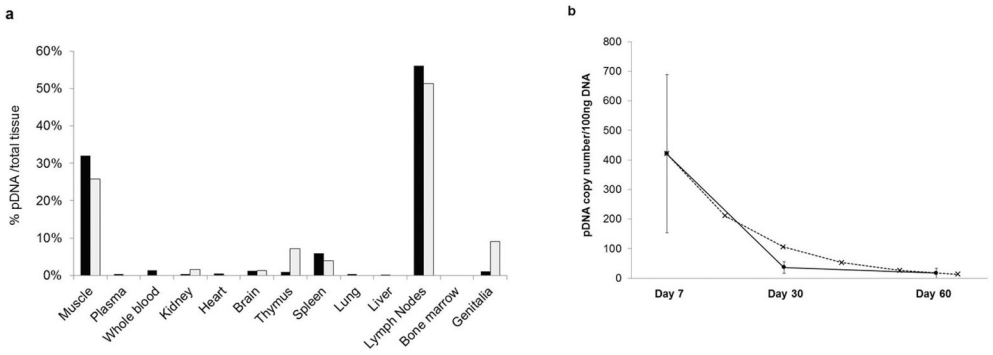

Figure 5. Tissue distribution of pDNA in New Zealand White Rabbits after topical pDNA/PEIm nanoparticle vaccination with DermaPrep.

(**a**) percentage of pDNA in 10 rabbits per test days (black bars: test day 7, grey bars: test day 30). (**b**) Average copy numbers of pDNA detected in the lymph nodes on days 7, 30 and 60 (circles and solid line). Calculated elimination rate of the nanoparticles from the lymph nodes (x and dashed line).

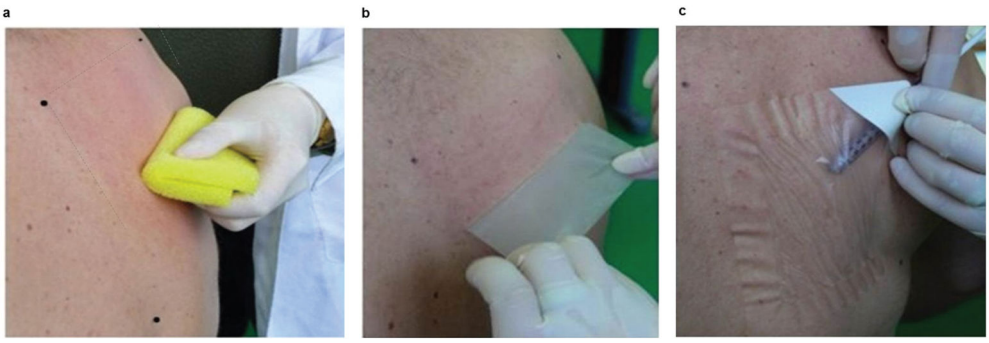

Figure 6. DermaPrep administration of liquid vaccine.

(**a**) The skin treatment starts with shaving and disinfection, then the body sponge is used to exfoliate the epidermis; (**b**) Tape stripping for the removal of the residual skin material (e.g.: dead cells); (**c**) Transparent film (the “patch”) designed to keep liquid vaccine in contact with the exfoliated epidermis for several hours without leaking. Liquid vaccine administered under the patch is completely dried after three hours, potentially improving the degree of penetration seen in earlier animal experiments where the liquid nanoparticles were dried within 30 minutes without the use of the patch.

Table 1.

Gene expression in LCs loaded *in vivo* with pDNA/PEIm nanoparticles

Material	Administration	% of fluorescent cells
Glucose	Transdermal	0.3
Nanoparticles	Transdermal	9.5
Nanoparticles	Injection	0.8
FITC-dextran	Iniection	15.9